PAPER • OPEN ACCESS

Analysis of the electrical and thermal behaviour of Li-ion batteries using 0D and 3D-CFD approaches with validation on experimental data

To cite this article: L Reina *et al* 2023 *J. Phys.: Conf. Ser.* **2648** 012044

View the article online for updates and enhancements.

Analysis of the electrical and thermal behaviour of Li-ion batteries using 0D and 3D-CFD approaches with validation on experimental data

L Reina[1], C Grigore[1], G Cicalese[1] and S Fontanesi[2]

[1] R&D CFD SRL, Via Tacito 59, 41123 Modena, Italy
[2] University of Modena and Reggio Emilia – DIEF Dipartimento di Ingegneria "Enzo Ferrari", Via Pietro Vivarelli 10, 41125 Modena, Italy

E-mail: luca.reina@red-cfd.it

Abstract. Due to their characteristics, lithium-ion cells are the reference in the construction of a battery pack for electric vehicles (EVs). Despite this, their use is strongly affected by the operating temperature because the materials they are made of are thermally stable only in a relatively limited range around ambient temperature. Cell modelling and simulation become therefore essential in the design of the cell, of the battery pack and of its auxiliary systems to optimize performance while maintaining sufficient safety margins.

In the present study, two zero-dimensional equivalent circuit models of a commercial Li-ion cell are developed and tuned in order to predict the electrical and thermal behaviour of the cell. The models are validated and compared with experimental data found in the scientific literature referring to both dynamic and static tests. This comparison shows the importance of tuning the model parameters, which are decisive for the accuracy of the simulation.

Using a commercial tool dedicated to battery modelling, a three-dimensional model is then developed to investigate the electrical and thermal behaviour of the cell from a spatial point of view. The results obtained are aligned with those found in the scientific literature.

With the present work, it has been possible to simulate and analyse the global behaviour of the cell (0D model) as well as its detailed behaviour (3D model) using relatively modest computational resources, thus constituting a solid base for more complex modelling such as that of a battery pack and its cooling system.

1. Introduction

Global pollution and climate change are issues that, due to their effects on the planet, have gained increasing attention in recent years, as evidenced by stringent international legislation. The scientific world is working to respond to this new challenge and, in the automotive sector, the electrification (partial or total) of the powertrain is increasingly consolidating as a possible solution to the problem.

The battery pack thus becomes the vehicle primary energy source. Lithium-ion cells represent the most widespread solution for its construction as they are secondary cells characterized by a high-power density, a high specific energy and a higher nominal voltage than the other cells available on the market. Furthermore, they have a very low self-discharge rate when not in use and are free from memory effect, essential characteristics for automotive applications.

Although these characteristics make them the current reference for the creation of a battery pack, they are not free from problems. Their use is limited by the operating temperatures which, if too hot, not

only degrade their performance and reduce the lifecycle, but can cause real safety problems for the end user. The materials they are made of are thermally stable only in a certain temperature range beyond which a series of chain exothermic chemical reactions are activated leading to the destruction of the cell, producing smoke, fire or violent cell venting. This phenomenon is known as thermal runaway and is a major concern in the design of a battery pack.

The electrochemical and thermal modelling and simulation of the cells therefore become fundamental in the design of the cells, of the battery pack and of its auxiliary systems.

Models characterized by a different level of detail and simulation time are available in the scientific literature. These can be grouped into three main categories [1]:

- physical models
- empirical models
- abstract models

Physical models (also known as white boxes) are models with a very high degree of detail [2]. They consider the physical structure of the cell materials and describe: the complex electrochemical processes, the thermodynamic phenomena, the chemical kinetic phenomena of the active species and the transport phenomena. With these models, therefore, all the processes that take place inside the active materials of the electrodes and the electrolyte are simulated. For this reason and for the high degree of detail of the model, a large number of parameters as well as a deep knowledge of the physical characteristics of the materials are required. Furthermore, a high computational cost for the resolution of the interdependent differential equations is needed, in fact those types of models are generally used only at the single cell design level [1].

Empirical models (also known as black boxes) cannot give a deep insight into the system [1] since they are based on a transfer function between the system experimental output and input data. For this reason, those types of models are easier to configure and are able to give quick responses [1] but however their accuracy is limited [2].

Abstract models (also known as grey boxes) do not provide a physical representation of the cell but a different and equivalent one [1]. The most common is the equivalent circuit model [3-6]. This modelling logic is simple and practical because it allows to replace the complex electrochemical phenomena which occur inside the cell with an equivalent electrical circuit without excessively compromising the accuracy of the results [1,6]. Furthermore, those models guarantee a significantly reduced computational effort compared to a physical model.

The equivalent circuit which models the cell is made up of three main components:

- an ideal voltage source which models the Open-Circuit Voltage (OCV) of the cell.
- a resistor which models the static behaviour of the cell.
- one or more RC groups (a resistor and a capacitor connected in parallel) which model the dynamic behaviour of the cell.

Increasing the number of RC groups increases both the accuracy and the complexity of the model [5,6]. The RC groups elements value are typically called dynamic parameters and are essential for the accuracy of the simulation.

This work presents an electrical and thermal analysis of a cylindrical LFP ($LiFePO_4/Graphite$) cylindrical cell using 0D and 3D-CFD approaches. In particular, two zero-dimensional equivalent circuit models are developed and tuned using the two commercial software MATLAB-Simulink-Simscape licensed by Mathworks and Simcenter Battery Design Studio licensed by Siemens DISW. The models are used to predict the electrical and thermal behaviour of the cell. The obtained results are compared with experimental data found in the scientific literature to validate the models. Then, a three-dimensional model is developed using the commercial software Simcenter STAR-CCM+ licensed by Siemens DISW to investigate the electrical and thermal behaviour of the cell from a spatial point of view, predicting the temperature distribution inside the cell and the most stressed component.

2. 0D modelling

Two zero-dimensional (0D) equivalent circuit models are developed and compared to highlight pros and cons of different approaches. The experimental dataset used to develop and validate the 0D models is available in [7] and it contains two sets of experimental data for a wide range of temperatures:

- Static tests at low C-rates ($C/30$).
- Dynamic tests referring to the current profile obtained from the Urban Dynamometer Driving Schedule (UDDS) driving cycle.

By means of the provided MATLAB scripts in [7] it is possible to determine the OCV curve and the dynamic parameters of the cell based on the outcomes of the experimental tests.
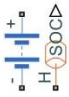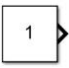
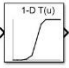### 2.1. MATLAB-Simulink-Simscape model

The equivalent circuit model of the cell created using the Battery Module of MATLAB-Simulink-Simscape is shown in Figure 1.
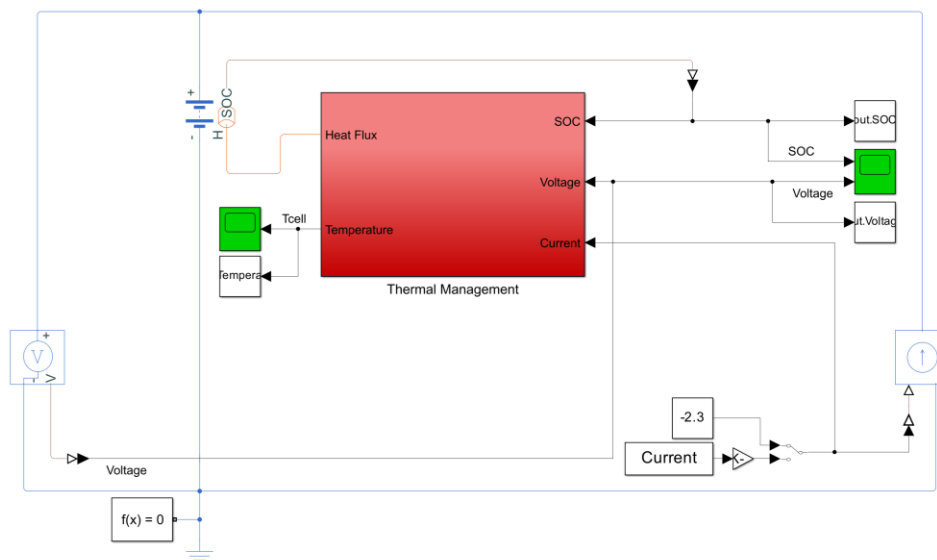
Figure 1. MATLAB-Simulink-Simscape cell model.

The main blocks used in the model are described in Table 1.

Table 1. Representation and description of the main blocks used in the model.

Block symbol	Block name	Block description
	Battery (Table-based)	It models a battery based on tabulated characteristics as functions of state-of-charge, SOC, and optional temperature, T.
	Controlled Current Source	It represents an ideal current source that is powerful enough to maintain the specified current through it regardless of the voltage across it.
	Voltage Sensor	The block represents an ideal voltage sensor, that is, a device that converts voltage measured between any electrical connections into a physical signal proportional to the voltage.
	Constant	It outputs a constant value specified by the user.
	Lookup Table (1-D)	It performs n-dimensional interpolated table lookup including index searches. The table is a sampled representation of a function in N variables
	Controlled Heat Flow Rate Source	It represents an ideal energy source in a thermal network that can maintain a controlled heat flow rate regardless of the temperature difference.
	Temperature Sensor	It measures temperature in a thermal network. There is no heat flow through the sensor.

The model fundamental element is the battery block which contains the parameters of the cell and those of the equivalent circuit.

The following criteria are adopted in the configuration of the block:
- three RC groups are used.
- the thermal flow input port is activated to account for the temperature variation of the cell which is modelled as a thermal mass.
- the dependence of the cell parameters on the temperature is not considered as temperature differences are less than $5°C$.

The battery block is electrically connected to a controlled current source block and to a voltage sensor block. The former is used to impose a custom current profile, while the latter is used to measure the voltage of the cell.

The thermal model is implemented in the subsystem called thermal management (see Figure 2) which uses the Bernardi equation to predict the heat generated from the cell [8]:

$$\dot{Q}_{gen} = I(OCV - V) - IT\frac{\partial OCV}{\partial T}$$

(1)

where: I is the cell current $[A]$; V is the cell terminal voltage $[V]$; T is the cell temperature $[K]$ and $\frac{\partial OCV}{\partial T}$ is the temperature derivative of the cell open-circuit voltage (also known as entropic coefficient) $[V/K]$. Furthermore:
- $I(OCV - V)$ is the *irreversible* heat generation term due to Joule heating and electrode overpotentials [8].
- $IT\frac{\partial OCV}{\partial T}$ is the *reversible* heat generation term due to entropy change [8].
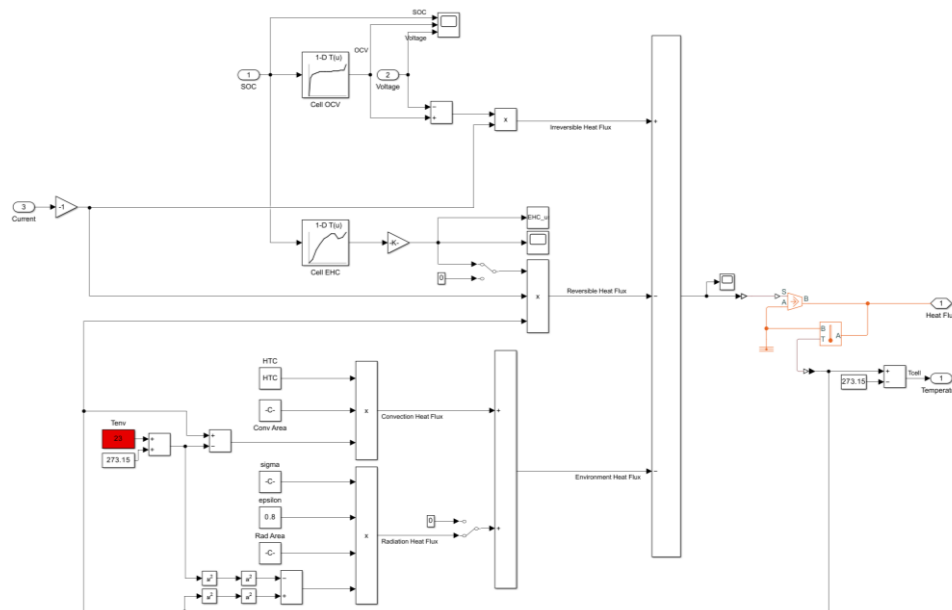
Figure 2. MATLAB-Simulink-Simscape cell thermal model.

In particular, the net heat to which the cell is subjected is determined by the sum of the gross heat generated from the cell and the heat exchanged with the environment by convection and radiation. The irreversible heat generation term of the Bernardi equation is calculated implementing the Open-Circuit Voltage as a function of the State of Charge (SOC) in a 1D lookup table and using the simulated cell voltage measured with the voltage sensor and the current of the controlled current source.

The reversible heat generation term of the Bernardi equation, instead, is calculated using the current of the controlled current source as well as the simulated cell temperature measured by the temperature sensor and implementing the entropic coefficient as a function of the SOC in a 1D lookup table [9]. The used entropic coefficient is shown in Figure 3.
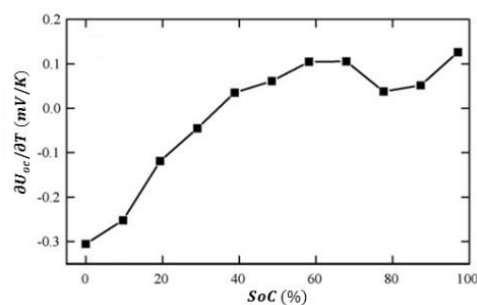
Figure 3. Entropic coefficient used in the model.

Lastly, the heat exchanged with the environment is calculated implementing the convective heat transfer coefficient, the emissivity of the cell, the Boltzmann constant, the heat transfer surface area of the cell and the ambient temperature within constant blocks and using the simulated cell temperature measured with the temperature sensor.

Main cell parameters are reported in Table 2.

Table 2. Main cell parameters.

Parameter	Value
Cell mass [kg]	0.07
Nominal capacity [Ah]	2.3
Minimum voltage[V]	2.3
Maximum voltage [V]	3.6
Specific heat [J/kg K]	848
Heat transfer surface area [m^2]	0.0064

2.2. Simcenter Battery Design Studio model

Simcenter Battery Design Studio (BDS) models the cell components from a geometrical, chemical and thermal point of view necessitating the specification of a large number of parameters. Since those measurements are not available, most of the data are referenced to the cell datasheet and to the papers [10-18]. An insight on how the analysed battery is made is reported in Figure 4.

Dynamic parameters of the three RC groups are computed by means of an internal regression tool based on the same experimental data discussed previously.

The process followed for the realization of the components of the cell and their assembly impact on cell behaviour and they can be taken into account by BDS, which modifies some dimensions accordingly to machining process of the battery.
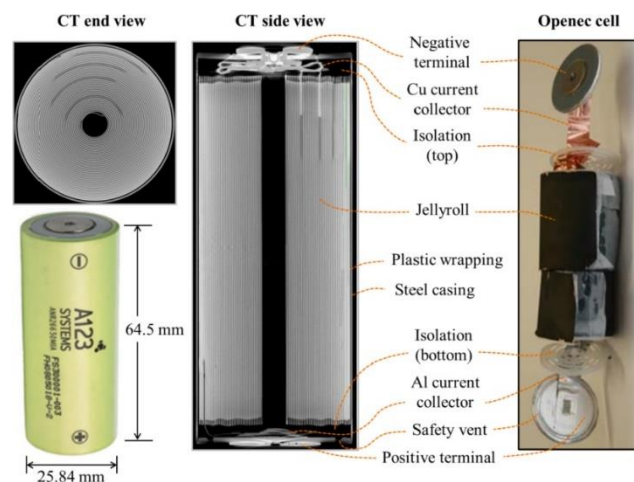
Figure 4. Details of cell construction and constituting components: actual cell along with CT scans (left) and uncased cell (right) [12].

2.2.1. Cell construction

The positive electrode current collector is an aluminium sheet having a thickness of $20 \, \mu m$ [10] and a height of $55.5 \, mm$ [16] of which it has been estimated that $52 \, mm$ are coated with a layer of active material. It has a heat capacity of $0.897 \, J/g \cdot K$ and a thermal conductivity of $237 \, W/m \cdot K$ [10]. The electrode length is automatically calculated by the software once the internal and external diameter dimensions of the jellyroll are defined. It was assessed that the 4 electrode tabs were made with typical material and dimensions for the typology of the analysed cell, that is aluminium with a width of $8 \, mm$ and a thickness of $90 \, \mu m$.

The layer of the positive electrode active material has a thickness of $70 \, \mu m$ and is made of $LiFePO_4$ having a heat capacity of $0.8 \, J/g \cdot K$ and a thermal conductivity of $1.48 \, W/m \cdot K$ [10]. In detail, the

layer is composed, in weight fraction, of 90% of $LiFePO_4$ with the addition of 2% of PVDF as a binder and 8% of graphite as a conductivity aid.

For the electric potential of the positive electrode the equation 2 from [17] is used:

$$U_{pos} = 3.4323 - 0.4828\,exp(-80.2493(1-y)^{1.3198})$$
$$- 3.2474 \times 10^{-6}\,exp(20.2645(1-y)^{3.8003})$$
$$+ 3.248 \times 10^{-6}\,exp(20.2646(1-y)^{3.7995})$$

$$(2)$$

The negative electrode current collector is a copper sheet having a thickness of $12.4\,\mu m$ [10] and a height of $57.5\,mm$ [16] of which it has been estimated that $54\,mm$ are coated with a layer of active material. It has a heat capacity of $0.396\,J/g \cdot K$ and a thermal conductivity of $398\,W/m \cdot K$ [10]. As for the positive electrode, the length is automatically calculated by the software once defined the dimensions and the assembly process of the jellyroll. It was assessed that the 4 electrode tabs were made with typical material and dimensions for the typology of the analysed cell, that is nickel with a width of $8\,mm$ and a thickness of $90\,\mu m$.

The increased height of the active material coating of the negative electrode is necessary to prevent lithium plating during fast recharging [16].

The electrode active material layer has a thickness of $34\,\mu m$ and is made of LiC_6 having a heat capacity of $0.641\,J/g \cdot K$ and a thermal conductivity of $1.04\,W/m \cdot K$ [10]. In detail, the layer is composed, in weight fraction, of 93% LiC_6 to which is added 7% of CMC as a binder.

For the electric potential of the negative electrode equation 3 from [17] is used:

$$U_{neg} = 0.6379 + 0.5416\,exp(-305.5309x) + 0.044\,tanh\left(-\frac{x-0.1958}{0.1088}\right)$$
$$- 0.1978\,tanh\left(\frac{x-1.0571}{0.0854}\right)$$
$$- 0.6875\,tanh\left(\frac{x-0.0117}{0.0529}\right) - 0.0175\,tanh\left(\frac{x-0.5692}{0.0875}\right)$$

$$(3)$$

The separator is a polymer membrane having a thickness of $25\,\mu m$, a density of $0.9\,g/cm^3$, a heat capacity of $1.883\,J/g \cdot K$ and a thermal conductivity of $0.5\,W/m \cdot K$ [10].

The porosity, which for Li-ion cells is typically between 40% and 60%, was estimated as 54%.

The electrolyte is composed of $LiPF_6$ lithium salt, having a molality of $0.8\,mol/kg$, dissolved in a solution of:

- ethylene carbonate (EC)
- propylene carbonate (PC)
- dimethyl carbonate (DMC)

with EC/PC/DMC concentration of 31:10:59 by weight and 27:9.7:63.3 by volume [10].

The heat capacity is $1.2\,J/g \cdot K$.

The cell assembly process requires the definition of the dimensions of the cylindrical mandrel around which to roll up the jellyroll, of the position of the electrodes and of their offset, of the separator length and of its overlap with the electrodes. Therefore, we define the geometrical dimensions of:

- mandrel, diameter of $4.4\,mm$ [12].
- jellyroll, outer diameter of $24.84\,mm$ [12].

- electrodes and separator, separator feed length of $10\ mm$, separator tail length of $70\ mm$, overlap at start of $3\ mm$ and overlap at end of $32\ mm$.

2.2.2. Comparison with the actual cell

The comparison between the model and the cell datasheet in terms of electrical properties is shown in Table 3. It is possible to see that the differences between the model and the real cell are less than 1%.

Table 3. Model-datasheet electrical parameters comparison.

Parameter	Model	Datasheet	Difference [%]
Capacity [Ah]	2.32	2.3	0.87
Nominal voltage [V]	3.27	3.3	0.91

The qualitative comparison between the modelled jellyroll and the real one [16] is illustrated in Figure 5. It is possible to observe a substantial correspondence of their geometric characteristics.
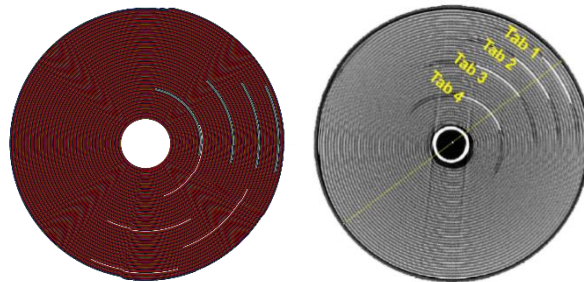
**Figure 5.** Modelled jellyroll (left) and jellyroll of the real cell (right).

2.3. Simulations

The developed models are tested to compare the result of the simulation with the experimental data of the cell. In particular, two test typologies are used:

- dynamic test, in which the current profile is obtained from the UDDS driving cycle and repeated several times until the lower cut-off cell voltage is reached.
- static test, with a constant discharge current of $C/1$.

2.3.1. Dynamic test

The cell was tested using the current profile available in the experimental data and represented in Figure 6. It consists of an initial constant current discharge and of a subsequential repetition of the UDDS driving cycle normalized current.
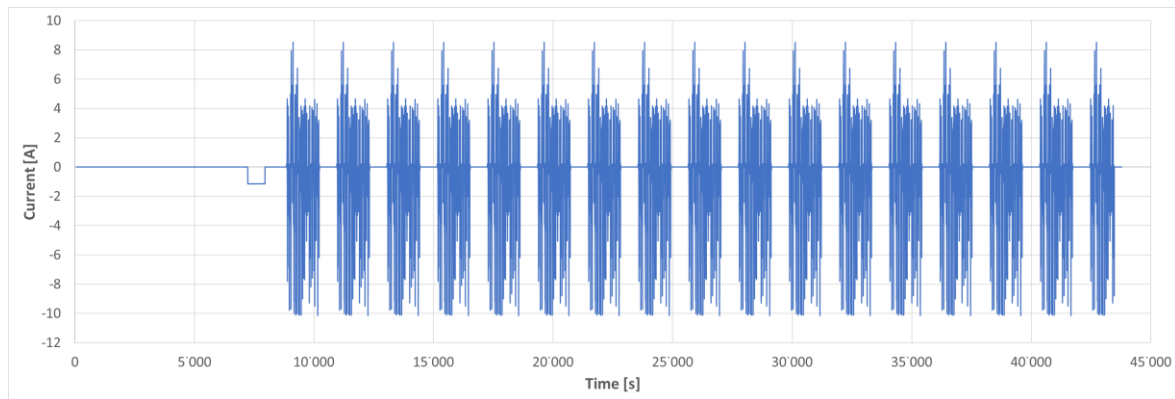
Figure 6. Dynamic test current profile.

The comparison of the electrical response of the models with the experimental data, represented in Figure 7, shows that the *BDS model* is the one that reproduces the experimental voltage profile most accurately. In detail, the *Simscape model* reproduces only the voltage response to the initial current step. The accuracy of the response is evaluated in terms of root-mean-square error (RMSE) which for the *Simscape model* is $97.08 \ mV$ while for the *BDS model* is $19.13 \ mV$.
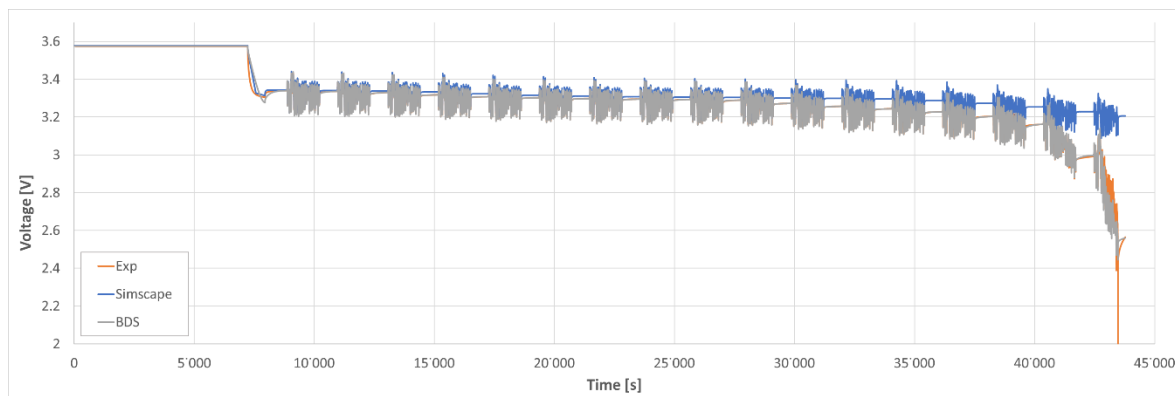
Figure 7. Comparison of the electrical response of the models with the experimental data.

Since no information are available on the thermal boundary conditions of the experimental data, some assumptions are introduced in the model calibration:

- forced convection with a convective heat transfer coefficient (HTC) of $100 \ W/m^2 \cdot K$.
- cell emissivity of $0.8 \ W/m^2$, a typical value for a coated cell.
- ambient temperature of $25.7°C$, the average value to which the cell temperature tends when no current is applied.
- initial cell temperature of $25.64°C$, the cell temperature value measured in the first sampling instant.
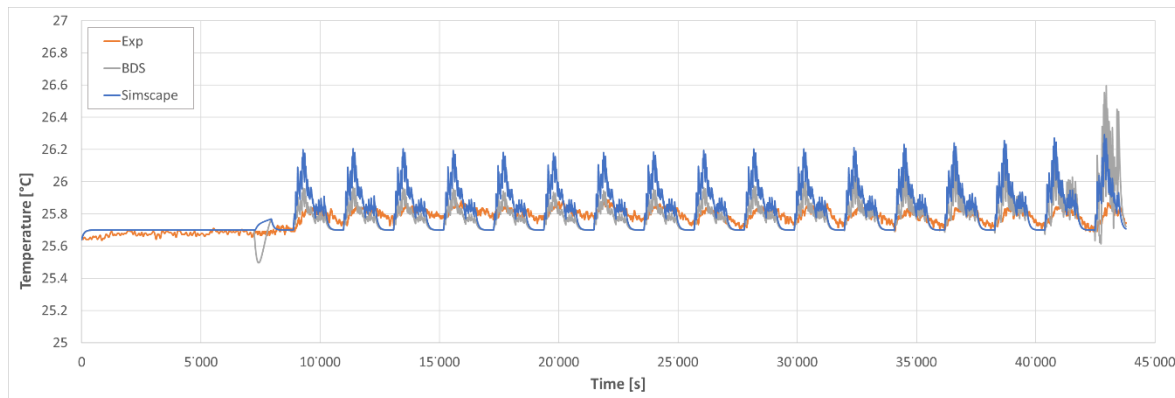
The comparison of the thermal response of the models with the experimental data is represented in Figure 8.

The accuracy of the simulation can be evaluated positively despite the difference between the temperature profiles, due to the following:

- in the Bernardi equation, the irreversible heat generation term is equal to the difference between the open circuit voltage and the simulated voltage of the cell; consequently, a greater deviation of the latter from the OCV corresponds to a more intense generated heat and an increase in cell temperature. This is evident in the initial and final parts of the simulation.

- the different rates of temperature variation between the models and the experimental data can be attributed to different thermal dynamics between the simulated cell and the actual one. Although the c_p used is the one calculated automatically by BDS, and it is consistent with the value found in the papers used for modelling, it was not possible to obtain a trend similar to the experimental one even doubling its value.
- in the Bernardi equation, the reversible heat generation term varies with the opposite sign with respect to the entropic coefficient. Referring to the used entropic coefficient (see Figure 3), it is negative up to approximately 35% of SOC and positive for the remaining interval. Thus, in the initial part of the simulation (when the cell is charged), the entropic contribution tends to cool the cell, while in the final part (when the cell is discharged) it tends to heat it, amplifying the already marked difference in temperature between the models and the experimental data.

The accuracy of the thermal response is evaluated in terms of RMSE which for the *Simscape model* is $0.113°C$ while for the *BDS model* is $0.088°C$.
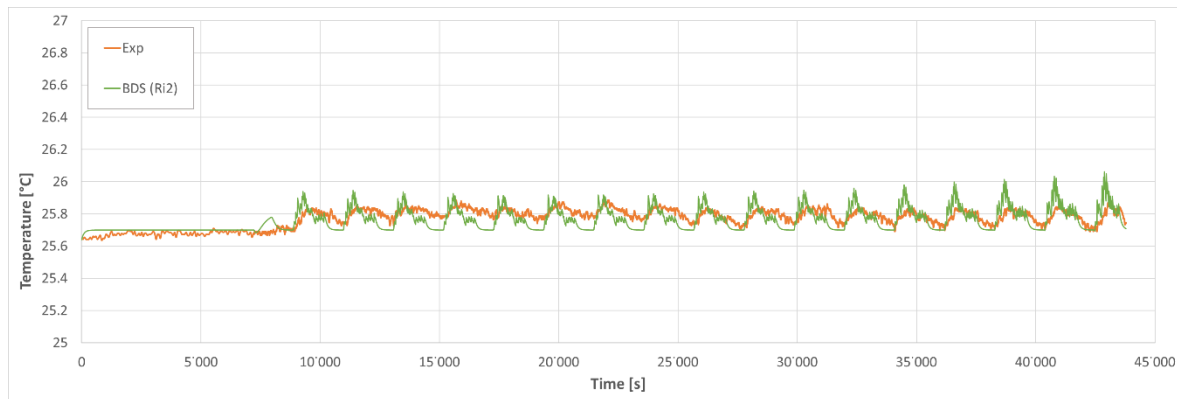

Figure 8. Comparison of the thermal response of the models with the experimental data.

To reduce the dependence of the thermal response on the simulated voltage, a different calculation method of the irreversible heat generation term of the Bernardi equation is used. In particular, the irreversible term is no longer calculated as the difference between the OCV and the simulated voltage but as the Joule effect (Ri^2) on the equivalent circuit resistors.

The evaluation is performed only with the *BDS model* since it gives the most accurate results with respect to the experimental data in terms of voltage response.

The comparison of the thermal response of the model thus configured with the experimental data is shown in Figure 9. Although the considerations listed above are still valid, the simulated response is improved as demonstrated by the lower RMSE of $0.062°C$.
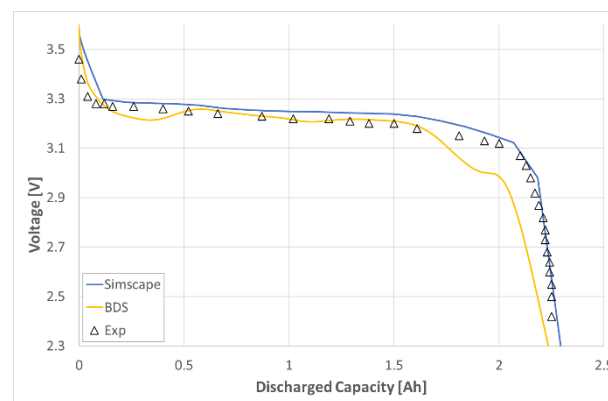
Figure 9. Comparison of the thermal response of the *BDS model* (Ri^2) with the experimental data.

2.3.2. Static test

The cell is tested using a $C/1$ ($2.3A$) constant current profile. In this case, the experimental data are obtained from [13].

The comparison of the electrical response of the models with the experimental data, represented in Figure 10, shows how, differently from what was observed with the dynamic test, the electrical response of the *Simscape model* is more accurate with respect to the experimental data. Furthermore, the electrical response of the *BDS model* is an evident example of how the result of an equivalent circuit model is strongly conditioned by the methodology used for determining its dynamic parameters.

The accuracy of the response is evaluated in terms of RMSE which for the *Simscape model* is $52.25\ mV$ while for the *BDS model* is $184.08\ mV$.
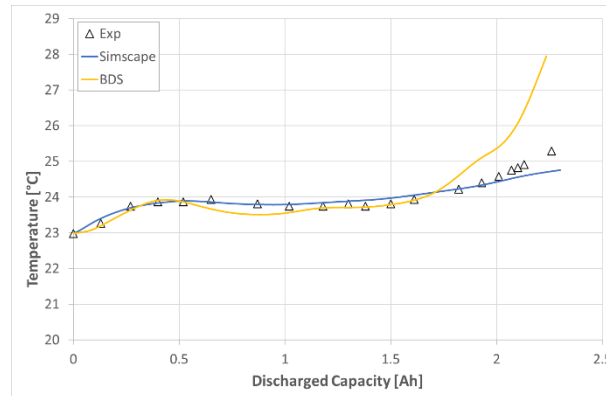

Figure 10. Comparison of the electrical response of the models with the experimental data.

Since no information are available on the thermal boundary conditions of the experimental data, some assumptions are introduced for this test as well:

- forced convection with a convective heat transfer coefficient (HTC) of $35\ W/m^2 \cdot K$.
- cell emissivity of $0.8\ W/m^2$.
- ambient and initial temperature of $23°C$.

The comparison of the thermal response of the models with the experimental data is shown in Figure 11. With reference to the irreversible heat generation term of the Bernardi equation, it is expected that the thermal response of the *Simscape model* is much more accurate than the *BDS model* one. It can be observed that with the latter model, the greatest error in the thermal response is in correspondence with the final part of the simulation where the simulated voltage differs most from the

experimental one. The accuracy of the response is evaluated in terms of RMSE which for the *Simscape model* is $0.182°C$ while for the *BDS model* is $0.843°C$.

Figure 11. Comparison of the thermal response of the models with the experimental data.

Using an approach similar to the one used for the dynamic test, the thermal response of the *BDS model* is evaluated using a different calculation method of the irreversible heat generation term of the Bernardi equation. The comparison of the thermal response of the model thus configured with the experimental data is shown in Figure 12. There is a clear improvement in the accuracy of the response in the final part of the simulation. Using this approach, the RMSE decreases to the value of $0.443°C$.
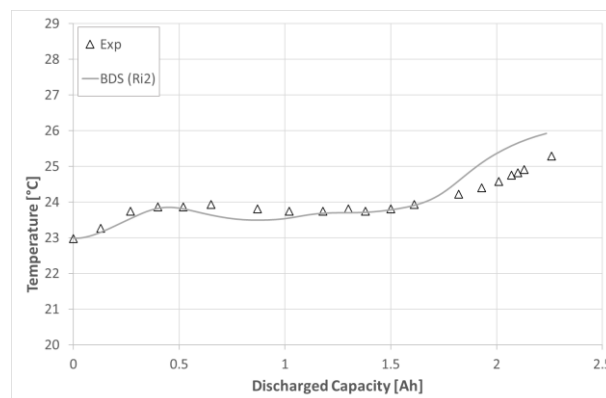
**Figure 12.** Comparison of the thermal response of the *BDS model* (Ri^2) with the experimental data.

3. 3D modelling

Upon the development of the 0D model, the study is extended by performing a three-dimensional analysis of the cell developing a 3D model.

For the cell modelling the commercial software Simcenter STAR-CCM+ is used and, specifically, the Battery Simulation Module which allows the simulation of the electrical and thermal response of the cell. If the cell jellyroll modelled in BDS is available, this module allows its import, limiting the 3D modelling just to the other components. For the development of the model, the information contained in the cell datasheet and in the papers mentioned in paragraph 2.2 are used.

3.1. Cell geometry

The geometry of the cell was reproduced, except for the jellyroll, by referring to Figure 4. The main components are shown in Figure 13.
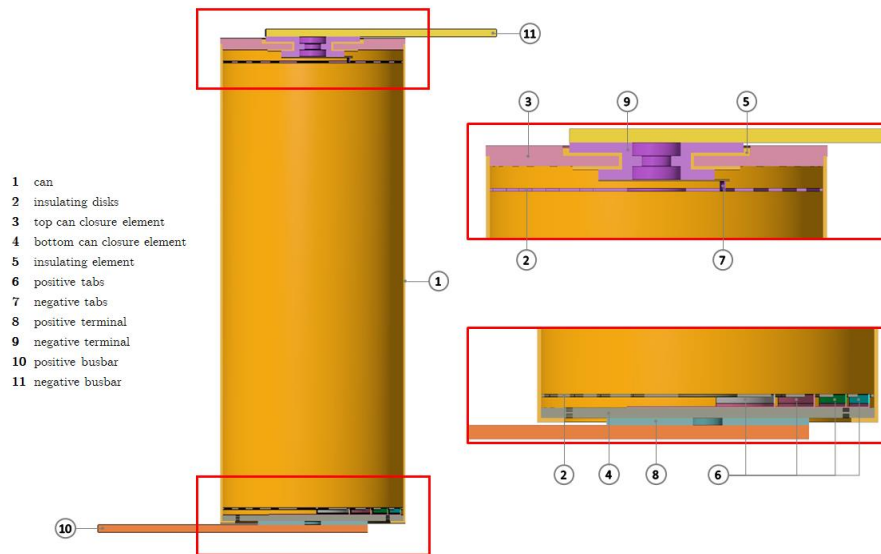
Figure 13. Modelled cell main components.

In the modelling of the cell geometry, considering the irrelevant effects on the solution, the following conditions are set:

- the thin insulating layer between the can and the jellyroll is neglected and replaced with an electrically insulating interface to simplify the mesh creation process.
- the dimensions of the safety vents are estimated since the real values were not found.
- the geometry of the connection between the various tabs is simplified.
- a generic geometry is adopted for the busbars.

The physical models for modelling the jellyroll and the remaining cell components allows the simulation of both thermal and electrical quantities inside the cell.

The BDS model discussed previously is imported in the current simulation framework to include all the information related to jellyroll geometry, chemical and thermal characteristics. It is worth noting that the heat generated by the jellyroll is computed by means of its electrochemistry behaviour defined in the BDS model, while the ohmic heating of the other cell components requires a specific model for the evaluation of the irreversible heat generation due to the current flow.

To allow the exchange of heat and current between different components, some interfaces are defined paying attention to those dealing with the jellyroll/can contacts and conductive/insulating materials, where low electrical conductivity is set.

For the definition of the mesh, several simulations were made using different meshes to understand the dependence of the simulation results on the geometry discretization and the major outcomes are here discussed for the sake of brevity. The cell was tested with a $6C$ constant current for 60 seconds to produce a high temperature variation in a relatively short simulation time. The results showed that there is not a high difference in temperatures as the mesh varies. It could be deduced a convenience in using coarse meshes even if some temperature gradients cannot be captured, especially near the contact area between components with very different dimensions as for example jellyroll-tabs.

For this reason, in order to obtain a refined geometric discretization of the cell with a reasonable number of cells, the results discussed hereafter are obtained with the mesh depicted in Figure 14 being a reasonable trade-off between accuracy and simulation time (considering that the longest simulation duration using a 12-core CPU is of about one week).
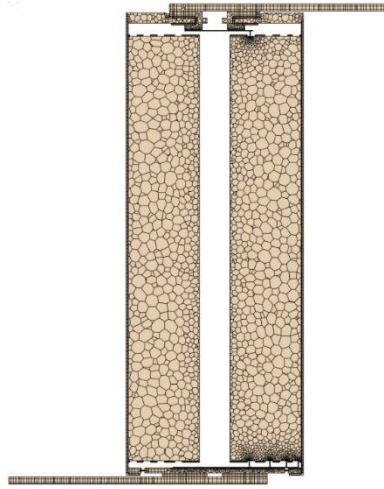
Figure 14. Section view of the mesh used for the simulations.

As for the boundary conditions, the following are used:
- *electric current* on the transversal surface of the positive busbar, to define the surface through which the current (positive or negative) enters the system.
- *electric potential* on the transversal surface of the negative busbar, to define the fixed potential surface through which the (positive or negative) current leaves the system.
- *convection* on the external surface of the can, to define the surface on which the heat exchange by convection takes place between the system and the environment.

3.2. Simulations

The 3D model is tested in the same way as the 0D one and two tests are performed:
- dynamic test, in which the current profile is obtained from the UDDS driving cycle.
- static test, with a constant discharge current of $C/1$.

For both tests, only the thermal response is evaluated since the electrical one depends solely on the typology of the used model (equivalent circuit model) and not on the dimension in which this is developed (0D or 3D).

3.2.1. Dynamic test

The dynamic test performed with the 0D model showed that the most accurate result with respect to the experimental data is obtained using the *BDS model* dynamic parameters values (see par. 2.3.1). For this reason, the same values are also used in the 3D model, importing into STAR-CCM+ the jellyroll modelled in BDS (see par. 3.2).

The dynamic test used, differently from the one used for the 0D model, consists of a single current profile obtained from the UDDS driving cycle since the simulation time is of about one week.

The thermal response of the model is evaluated in terms of:
- maximum, average and minimum temperature of the jellyroll (see Figure 15a).
- maximum and average temperature of the can (see Figure 15b).

The temperatures trend is similar to the ones of the zero-dimensional modelling, since the same considerations are still valid. The RMSEs calculated on the average temperatures are $0.086°C$ for the jellyroll and $0.062°C$ for the can.
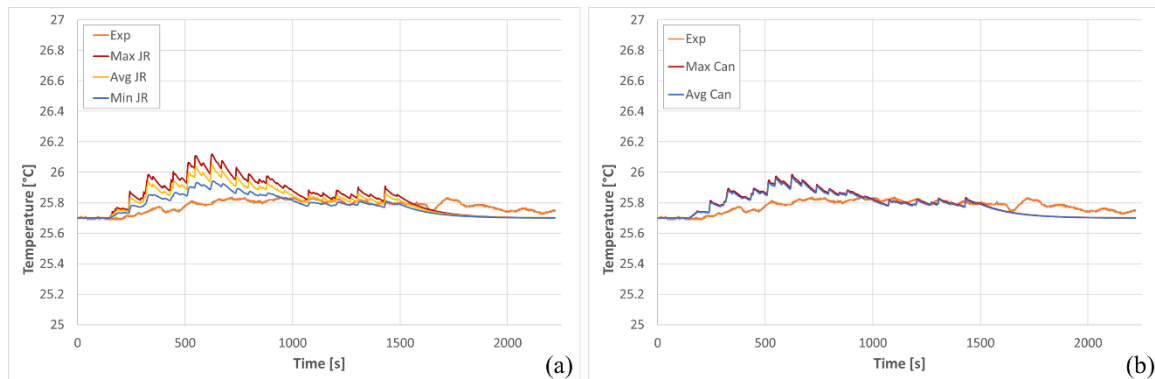
**Figure 15.** Comparison of the thermal response of jellyroll (a) and can (b) with the experimental data.

The temporal evolution of the temperature spatial distribution inside the cell is shown in Figure 16 every 180s. Since the test is dynamic and the convection is forced, the temperature varies rapidly over time. Furthermore, since the convective heat transfer is imposed on the external surface of the can, the lower thermal conductivity of the jellyroll in the radial direction compared to the axial one determines a temperature difference between its internal and external parts, thus generating a radial temperature gradient.
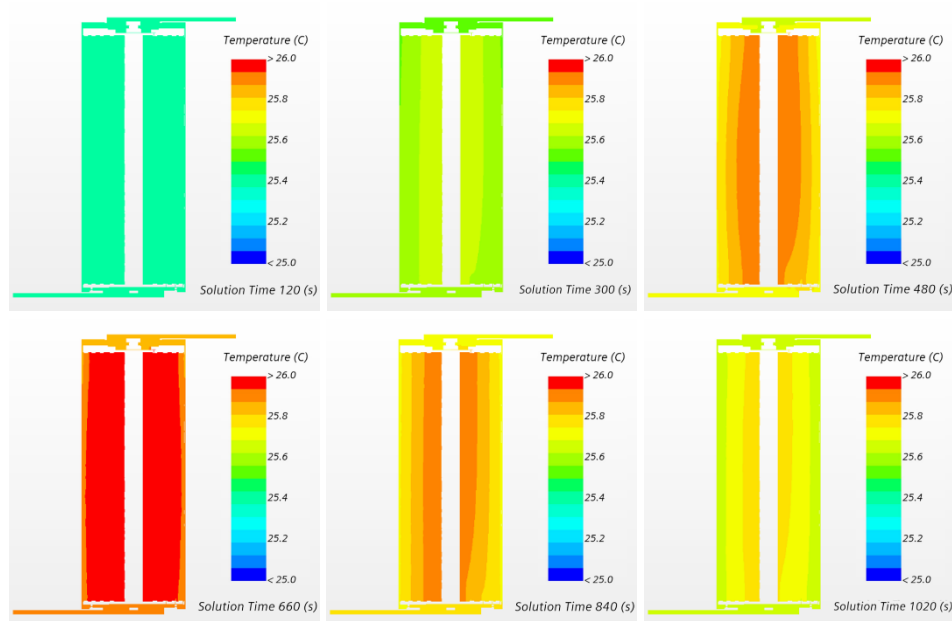
Figure 16. Temporal evolution of the temperature spatial distribution inside the cell.

It is also possible to observe a local temperature gradient in the axial direction near the tabs. This is more evident in Figure 17 which shows the temperature spatial distribution on the surface of both unrolled electrodes. The axial temperature gradient is determined by the presence of the tabs which, by exchanging heat with the jellyroll, cool down its contact surface.
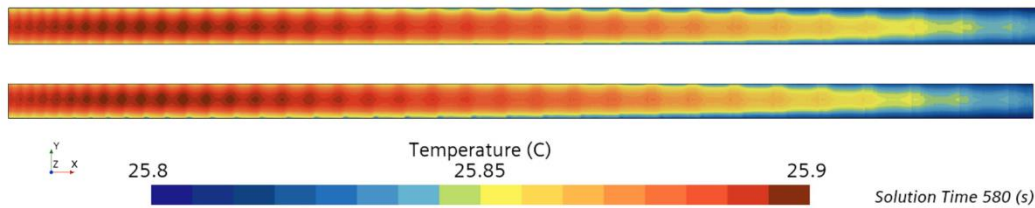
Figure 17. Temperature spatial distribution on the surface of negative (top) and positive (bottom) unrolled electrodes.

Due to their reduced thickness, tabs are the cell components in which is generated the highest current density and therefore the highest specific ohmic heat. In Figure 18 an example of one of the four negative tabs is shown.
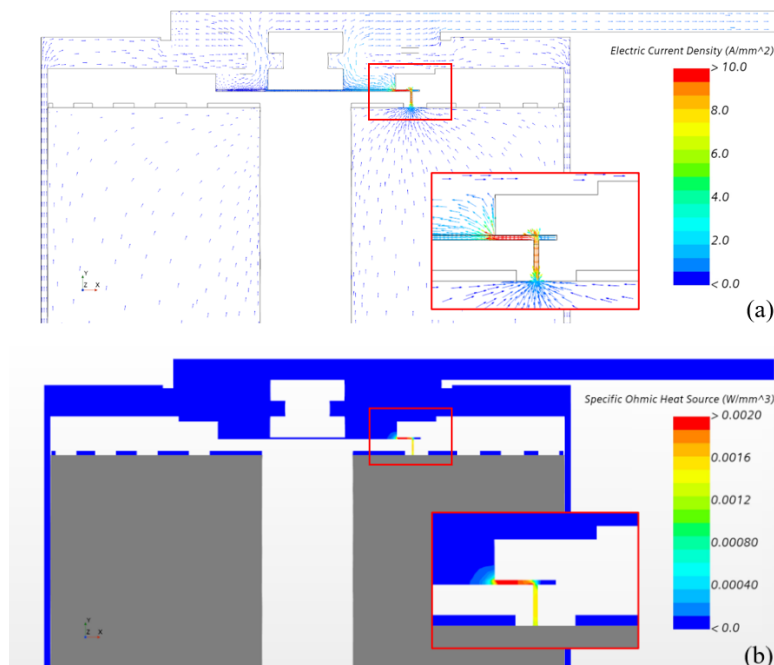
**Figure 18.** Current density (a) and specific ohmic heat (b) of a negative tab.

3.2.2. Static test

The static test performed with the 0D model shows that the most accurate result with respect to the experimental data is obtained using the *Simscape model* static parameters values. For this reason, for the 3D modelling of the cell, the jellyroll is entirely modelled in STAR-CCM+ instead of importing the one modelled in BDS which would have limited the choice of the dynamic parameters to its ones. The static test used, like the one used for the 0D model, consists of a constant discharge current of $2.3A$.

The thermal response of the model is evaluated in terms of:

- maximum, average and minimum temperature of the jellyroll (see Figure 19a).
- maximum and average temperature of the can (see Figure 19b).

Due to the temperature gradients discussed in the previous paragraph (see par. 3.2.1), a maximum temperature difference is generated inside the cell of about $1.5°C$, in line with the results reported in [10].
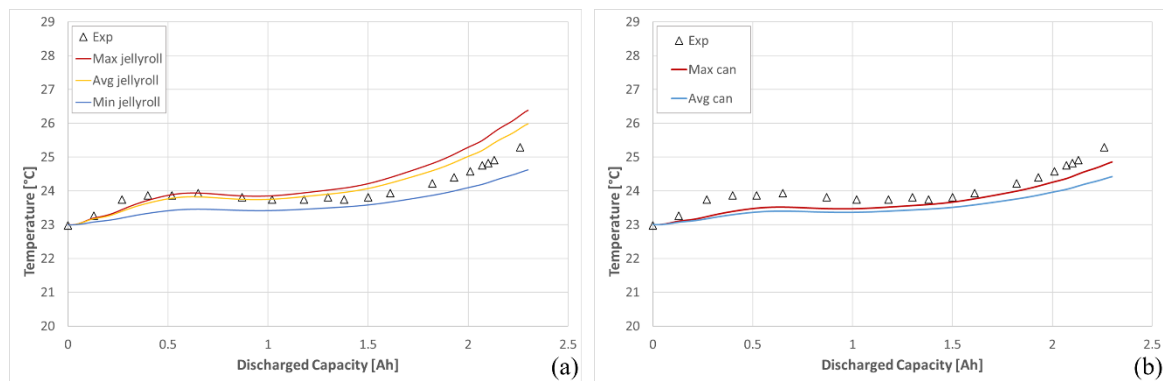
Figure 19. Comparison of the thermal response of the jellyroll (a) and can (b) with the experimental data.

4. Conclusions

With the present work, a practical methodology for system-level modelling of Li-ion battery cells is presented. At first a simple ECM implemented in Simulink is shown and then a more advanced approach using Battery Design Studio is implemented. The models allow to simulate the electrical and thermal response of the cell and to compare the results with those found in the scientific literature. Both approaches use empirical data to calibrate ECM parameters, but the latter also allows to compute cell electrical parameters starting from physical properties and give a rough estimate of the 3D effects occurring within the cell.

The paper shows in detail the methodology used to perform the simulations and the relative performance. The error in voltage prediction depends on the algorithm used for parameter optimization and the generalizability of the input data. Using the dynamic test parameters in a constant current discharge led to a larger error. Additional tests are planned to be performed using different current inputs to evaluate the generalizability of the calculated parameters.

From a thermal point of view, the results trend is the same of the electrical one. Since the thermal response is calculated with the Bernardi equation, it is directly dependent on the electrical one, indeed the lower the electrical RMSE, the lower the thermal one. To reduce this strict dependence, the calculation method of the irreversible heat generation term is changed reducing the thermal RMSE value by about 30% in the dynamic test and by about 50% in the static one.

Thanks to 3D detailed modelling, the temporal evolution of the temperature spatial distribution can be analysed allowing the identification of temperature gradients and of the most stressed components. Furthermore, it is possible to analyse the current density distribution and therefore to identify the areas of the cell in which more heat is generated due to Joule effect.

In conclusion, an equivalent circuit model is effective in simulating the cell behaviour only if accurate experimental tests are available to determine the dynamic parameters and to calibrate the model. Furthermore, the great versatility of an equivalent circuit model could be fundamental in the design and optimization of a battery pack, of its cooling system and of its management system (BMS).

References

[1]   Saidani F, Hutter F, Scurtu R-S, Braunwarth W and Burghartz J 2017 Lithium-ion battery models: a comparative study and a model-based powerline communication *Adv. Radio Sci.* **15** 83–91

[2]   Rao R, Vrudhula S and Rakhmatov D 2003 Battery modeling for energy-aware system design *IEEE Computer Society* **36** 77–87

[3]   Hu X, Li S and Peng H 2012 A comparative study of equivalent circuit models for Li-ion batteries *Journal of Power Sources* **198** 359–67

[4]   Rahmoun A and Biechl H 2012 Modelling of Li-ion batteries using equivalent circuit diagrams *Przeglad Elektrotechniczny* **88** 152–6

[5]   Huria T, Ceraolo M, Gazzarri J and Jackey R 2012 High fidelty electrical model with thermal dependence for characterization and simulation of high power lithium battery cells *IEEE International Electric Vehicle Conference* 1–8

[6]   Moss P L, Au G, Plichta E J and Zheng J P 2008 An electrical circuit for modeling the dynamic response of Li-ion polymer batteries *J. Electrochem. Soc.* **155** A986–94

[7]   Plett G L 2015 *Battery Management Systems: Volume 1, Battery Modeling* (Norwood: Artech House)

[8]   Jindal P, Katiyar R and Bhattacharya J 2022 Evaluation of accuracy for Bernardi equation in estimating heat generation rate for continuous and pulse-discharge protocols in LFP and NMC based Li-ion batteries *Applied Thermal Engineering* **201** 117794

[9]   Damay N, Forgez C, Bichat M-P and Friedrich G 2015 Thermal modeling of a large prismatic LiFePO$_4$/graphite battery. Coupled thermal and heat generation models for characterization and simulation *Journal of Power Sources* **283** 37–45

[10]   Li J, Cheng Y, Jia M, Tang Y, Lin Y, Zhang Z and Liu Y 2014 An electrochemical-thermal model based on dynamic responses for lithium iron phosphate battery *Journal of Power Sources* **255** 130–43

[11]   Ye Y, Shi Y and Tay A 2012 Electro-thermal cycle life model for lithium iron phosphate battery *Journal of Power Sources* **217** 509–18

[12]   Tahir W and Merten C 2022 Multi-scale thermal modeling, experimental validation, and thermal characterization of a high-power lithium-ion cell for automobile application *Energy Conversion and Management* **258** 115490

[13]   Prada E, Di Domenico D, Creff Y, Bernard J, Sauvant-Moynot V and Huet F 2012 Simplified electrochemical and thermal model of LiFePO$_4$-graphite Li-ion batteries for fast charge applications *J. Electrochem. Soc.* **159** A1508

[14]   Rad M S, Danilov D, Baghalha M, Kazemeini M and Notten P 2013 Thermal modeling of cylindrical LiFePO$_4$ batteries *Journal of Modern Physics* **4** 1–7

[15]   Ma Y, Teng H and Thelliez M 2010 Electro-thermal modeling of a Lithium-ion battery system *SAE International Journal of Engines* **3** 306–17

[16]   Rikka V R, Sahu S R, Chatterjee A, Prakash R, Sundararajan G and Gopalan R 2022 Enhancing cycle life and usable energy density of fast charging LiFePO$_4$-graphite cell by regulating electrodes' lithium level *iScience* **25** 104831

[17]   Safari M and Delacourt C 2011 Modeling of a commercial graphite/LiFePO$_4$ cell *J. Electrochem. Soc.* **158** A562–71

[18]   Zhang L, Lyu C, Hinds G, Wang L, Luo W, Zheng J and Ma K 2014 Parameter sensitivity analysis of cylindrical LiFePO$_4$ battery performance using multi-physics modelling *J. Electrochem. Soc.* **161** A762–76